Available online at www.sciencedirect.com
SCIENCE DIRECT®
Thermochimica Acta 446 (2006) 106–112
thermochimica acta
www.elsevier.com/locate/tca

High temperature mass spectrometric gas-release studies of kaolinite $Al_2[Si_2O_5(OH)_4]$ decomposition

K. Heide [a,*], M. Földvari [b]

[a] Institut für Geowissenschaften, Friedrich-Schiller-Universität Jena, Burgweg 11, D-07749 Jena, Germany
[b] Geological Institute of Hungary, Stefánia út 14 H-1143, Budapest, Hungary

Abstract

The evolution of hydrogen together with water release during dehydroxylation kaolinite was confirmed by means of simultaneous analysis of weight loss and evolved gases during a thermal treatment of kaolinite from different locations. The evolution of hydrogen during the dehydroxylation of kaolinite supports a specific structural arrangement of OH-ions during the decomposition.

A deficit in the vacuum weight loss can be explained by a degassing process at room temperature under high vacuum. Obviously approxmately 0.2 mol H_2O in the kaolinite structure are more mobile than OH-combined water release.

Together with the water release also carbon dioxide evolved also at the same temperature interval. The correlation to the dehydroxylation is obviously more an indication for a molecular fixation of CO_2, in the kaolinite structure, like the “indigenous” carbon, than an admixture of a carbonate mineral. The hydrocarbon release is independent of the hydrogen, CO_2, and water release.

In any cases small quantities of OH are fixed in the meta-kaolinite structure and still escape as H_2O still between 900 and 1200 °C.

Keywords: Kaolinite decomposition; Hydrogen release; MS analysis

1. Introduction

The dehydroxylation of kaolinite was studied in numerous papers [1–3]. The thermal decomposition of kaolinites is determined by different factors, such as degree of structural ordering, particle size and shape, adsorbed and substituted ions, mineral admixtures, etc. Also the influence of instrumental conditions on the decomposition rate is discussed in numerous studies [2].

The water release of kaolinite in a temperature range between 450 and 700 °C and the formation of the “meta-kaolinite” $Al_2Si_2O_7$ [4] is well-known:

$$Al_2[Si_2O_5(OH)_4] \Rightarrow Al_2[O_2\square/Si_2O_5] + 2H_2O \qquad (1)$$

In the thermogravimetric studies a discrepancy between the thermogravimetric weight loss (between 11.2 and 14.5 wt% [5,6]) and the theoretical value of 13.95 wt% is frequently reported. It was often explained by mineral admixtures like silica or smectite. But as shown by Bain and Morgan [7], the dehydroxylation of well-crystallized kaolinite begins at about 480 °C and increases rapidly to about 700 °C. The mass loss between 480 and 900 °C is 12.6%. That means the sample loss of 1.4 wt% H_2O before the typical dehydroxylation process was started.

The maximum temperature of dehydroxylation depends on the degree of disorder of the kaolinite structure [8,9].

Hindar et al. [5] show by thermosonic experiments, that the endothermic dehydroxylation is splitting into two separate processes (T_{max} ≈550 and ≈600 °C). The first step was explained due to the loss of “structural water” and a destruction of the kaolinite sheet structure. The second step was discussed as a kinetically controlled recombination of alumina and silica to the meta-kaolinite structure.

As discussed by Freund and Gentsch [10] and Freund et al. [11] the thermal dehydration of hydroxyl-containing compounds like kaolinite occurs in a formation of water molecules due to an interaction of neighbouring OH groups. The water release from the octahedral coordinated Al^{3+}-ion could generate isolated OH-groups.

The protons are less and less likely to form H_2O molecules. In the high-defect reaction product the formation of H_2 should be possible. In special studies about the gas release during the thermal treatment of kaolinite, the hydrogen formation was

---

[*] Corresponding author.
E-mail address: ckh@rz.uni-jena.de (K. Heide).

0040-6031/$ – see front matter © 2006 Published by Elsevier B.V.
doi:10.1016/j.tca.2006.05.011

confirmed [12], but the mechanism of H_2 evolution remained “obscure”.

The mass spectrometric gas-release studies can be used to study simultaneously the composition of evolved gases during the thermal treatment [13,14]. The present paper is focused on the detection of H_2O, CO_2, hydrocarbon fragments as CH and CH_3 and H_2 in a temperature range of RT up to 1450 °C.

In this temperature range also the transformation of the meta-kaolinite to an Al-Si-spinell occurs in an exothermal process between 900 and 1200 °C [4 p. 291].

2. Materials and experimental procedures

The kaolinite samples used in this study are both reference materials prepared under the auspices of the Clay Minerals Society and samples from kaoline deposits in Europe (Table 1). Dickite from Peru was used to compare the decomposition of two-sheet layer structure with different structural order evolved gas analysis was carried out by using a special high-temperature mass-spectrometer [15] in combination with a thermo-balance (STA 429 Netzsch). Measurements were performed under a vacuum of 10^{-3}–10^{-4} Pa using a constant heating rate of 10 K/min from RT to 1450 °C. The ion current for different mass/charge ratios ($m/z = 1200$) was recorded in a multiple ion detection (MID)-mode as a function of time by a quadrupole mass-spectrometer (QMA-125 Balzers AG). Temperature was controlled by a type S thermocouple at the bottom of the alumina crucible on the basis of ICTA-temperature reference materials.

The quantities of evolved gases were determined simultaneously with the mass loss. The lower limit of mass change is 0.001 mg. The accuracy of balance was tested with the decomposition of spec-pur–carbonates.

The degassing process occurs under highly non-equilibrium conditions. Volatile species are rapidly removed from the sample and, hence, the probability for reverse reactions between the volatiles and the melt can be avoided. Furthermore, interactions between the evolved gas species are minimized and a determination of the primary evolved species is possible. For the investigation we need about 10 mg of substances without any preparation.

Table 1
The chemical composition of kaolinite

	KGa-1[a] well-crystallized Georgia		KGa-2[a] poorly-crystallized Georgia		HI gem Dorfner	$Al_2[(OH)_4/Si_2O_5]$
	CL[b]	MH[c]	CL[b]	MH[c]		
SiO_2	45.0	44.2	44.2	43.9	48.5	46.55
TiO_2	1.58	1.39	2.17	2.08	0.36	
Al_2O_3	38.0	39.7	37.2	38.5	37.0	39.49
Fe_2O_3	0.26	0.13	1.14	0.98	0.25	
FeO	0.02	0.08	0.05	0.15	n.d.	
MnO	0.00	0.002	0.00	n.d.	n.d.	
MgO	0.02	0.03	0.04	0.03	n.d.	
CaO	0.02	n.d.	0.04	n.d.	n.d.	
BaO	n.d.	–	n.d.	–	0.08	
Na_2O	0.01	0.013	0.02	<0.005	0.05	
K_2O	0.04	0.05	0.02	0.065	0.08	
P_2O_5	0.05	0.034	0.06	0.045	0.11	
CO_2	n.d.		n.d.		n.d	
SO_3	n.d.		n.d.	0.02	n.d.	
F	0.013[d]		0.02		n.d.	
LOI 550 °C	14.31	12.6	14.24	12.6	12.99	13.96
550–1000 °C		1.18		1.17		
Σ	99.38	99.40	99.18	99.54		100.00
Kaolinite[e]	96.75% 45% SiO_2		95.03% 44.2% SiO_2		104.28%[d] 48.5% SiO_2	
$Water_{theo}$[f]	13.43%		13.15%		13.07%	
Kaolinite[g]	96.14% 38.0% Al_2O_3		94.12% 37.2% Al_2O_3		93.61% 37.0% Al_2O_3	
Mineralogical composition	Kaolinite 97% Anatas 2.5% Crandallite 0.5%		Kaolinite 95% Anatas 4%		Kaolinite 99% Silica	

---

[a] Van Ophen et al. [6].

[b] CL: Analyst: Clemency, Department of Geological Sciences, Buffalo, NY, USA.

[c] MH: Analyst: Haydn, Department of Geology, Bloomington, Indiana.

[d] Quartz admixture.

[e] Calculation of the kaolinite content on the basis of SiO_2-content.

[f] Calculation of the kaolinite content on the basis of Al_2O_3-content.

[g] Water content calculated on the basis of theoretical watercontent of 13.95%.

Table 2
Intensity of the ion current of H_2O-and CO_2-fragment ions in relation to the intensity of H_2O-molecule-ion m/z 18 (=100%) respectively, CO_2-molecule-ion m/z 44 (=100%) and the correlation coefficient R

	OH^+/H_2O^+ (m/z 17/m/z 18) R	O^+/H_2O^+ (m/z 16/m/z 18) R	H_2^+/H_2O^+ (m/z 2/m/z 18) R	H^+/H_2O^+ (m/z 1/m/z 18) R
Kieserite $MgSO_4H_2O$	29.93% 99.998%	3.421% 99.984%	0.343% 99.875%	6.785% 99.893%
	CO_2^+/H_2O^+ (m/z 44/m/z 18) R	CO^+/CO_2^+ (m/z 28/m/z 44) R	C^+/CO_2^+ (m/z 12/m/z 44) R	
Calcite $CaCO_3$ 0.5 mg	Without correltation	18.009% 99.445%	15.123% 99.993%	

The interpretation of the mass-spectra occurs on the basis of degassing profiles between RT and 1450 °C from the molecule ions of water ($H_2O^+ = m/z$ 18;), carbon dioxide ($CO_2^+ = m/z$ 44), and hydrogen ($H_2^+ = m/z$ 2) as well as by fragment ions of hydrocarbons ($CH^+ = m/z$ 13, and $CH_3^+ = m/z$ 15).

The separation of the hydrogen release from the water release is difficult because during the MS-detection of water the formation of fragments like $OH^+ = m/z$ 17; $O^+ = m/z = 16$; $H^+ = m/z$ 1 and $H_2^+ = m/z$ 2 in different intensities is possible.

We used as reference the decomposition of crystallohydrates as kieserite ($MgSO_4 \times H_2O$) between 250 and 400 °C to determine the fragmentation pattern of water molecule. The results of measurements are listed in Table 2. The ion current of fragment ions OH^+ (m/z 17), O^+ (m/z 16), H_2^+ (m/z 2) and H^+ (m/z 1) is given in relation to the ion current of the molecule ion H_2O^+ (m/z 18 = 100%) together with the correlation coefficients R. The characterization of water release by means of MS is possible with the molecule ion $H_2O^+ = m/z$ 18 or with the fragment ion $OH^+ = m/z$ 17. The >99.998% correlation between the intensity of m/z 18 and m/z 17 indicates the characteristic fragmentation mechanism of water molecule during the ionization process in the ion source. The following relation was determined (70 eV):

$$H^+ : H_2^+ : O^+ : OH^+ : H_2O^+ = 6.8 : 0.3 : 3.4 : 30 : 100.$$

The use of m/z 17 in the figures happens if the intensity of m/z 18 is outside of the measuring range. The determination of the fragmentation patterns during the decomposition of carbonate due to with spec-pure–carbonates. The relations between the intensity of fragment-ions and the intensity of the molecule ion CO_2^+ (=100%) are summarized in Table 2.

The relation between the ion–molecule intensity and the fragment ions are as following:

$$C^+ : CO^+ : CO_2^+ = 15.2 : 18.4 : 100$$

The maximum of decomposition rate of calcite under high vacuum conditions is determined at 563 °C. The negative mass loss at the beginning of decomposition is a repulsion phenomenon during the degassing in high vacuum [16].

3. Results

In the degassing profile and TG-curve of the standard kaoline KGa-1 the different-steps of decompositions are visible (Fig. 1).

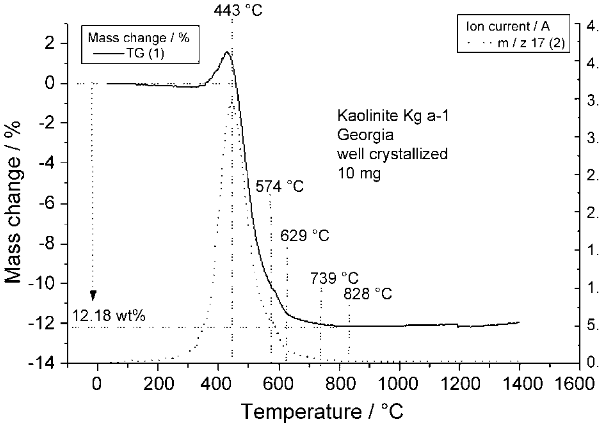

Fig. 1. Mass loss and water release of kaolinite standard KGa-1.

The mass loss of ≈1.70 mol H_2O is far from the theoretical loss of 2 mol H_2O, also after correction by means the drifting of the thermo-balance and on the basis of chemical analysis (s. Table 1 from the SiO_2-content 96.75% kaolinite are in the KGa-1 and we must expect a mass loss of 13.43 wt%). As shown in Figs. 2–4 CO_2, H_2, and hydrocarbons escaped during the heating treatment together with the water release, but sometimes with different temperatures of maximum degassing rate $\{CO_2\ T_{max} = 434\,°C$ (Fig. 2), water and hydrogen $T_{max} = 443\,°C$ (Fig. 3), hydrocarbons $T_{max} = 347\,°C$ (Fig. 4)$\}$.

Fig. 5 summarizes the TG curves of the different kaolinites.

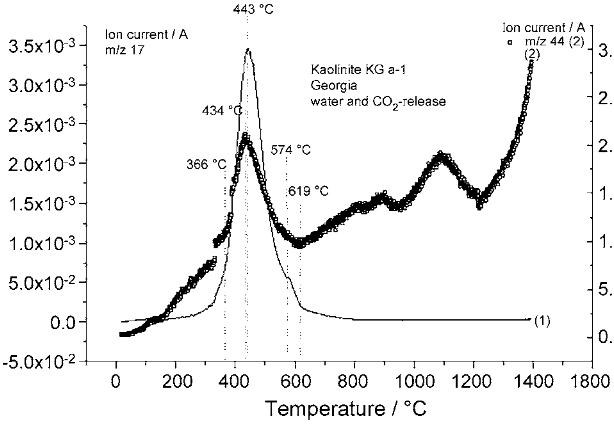

Fig. 2. CO_{2-} and H_2O release from kaolinite KGa-1.

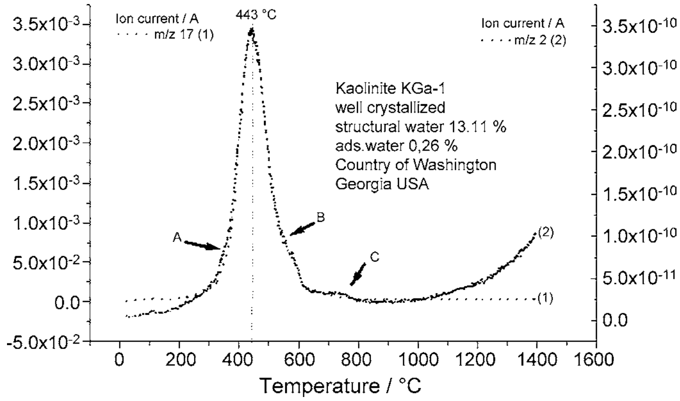

Fig. 3. H_2 and H_2O release from kaolinite KGa-1.

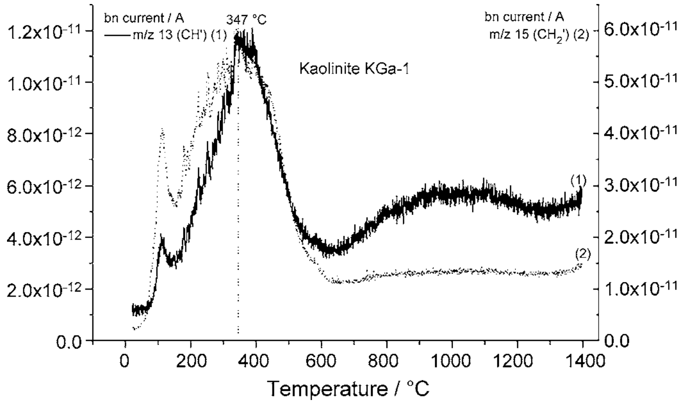

Fig. 4. CH^+ (m/z 13) and CH_3^+ (m/z 15) release from kaolinite KGa-1.

In Fig. 6 a detail of Fig. 3(B and C) is shown. The rate of hydrogen release is different to the rate of water release above 550 °C up to 850 °C.

The mass loss at temperatures of 1000 °C is, in general, significantly lower in relation to the theoretical mass loss by the stoichometry of kaolinite and can be explained by a water release at room temperature under high vacuum. These results confirmed the data in different references, e.g. [5,15].

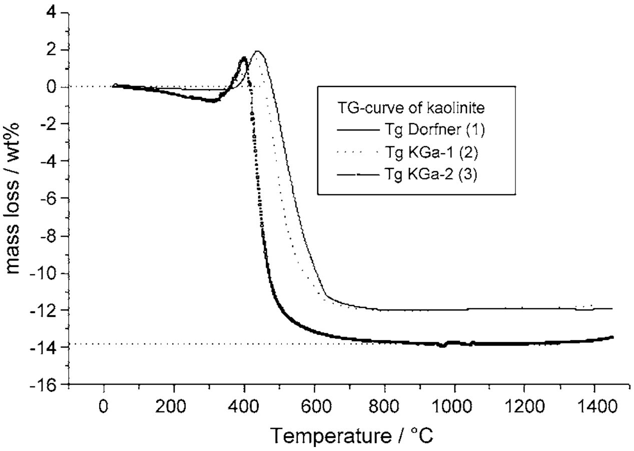

Fig. 5. Mass loss curves (TG-curves) of investigated kaolinites (sample weight, 10 mg; heating rate, 10 K/min).

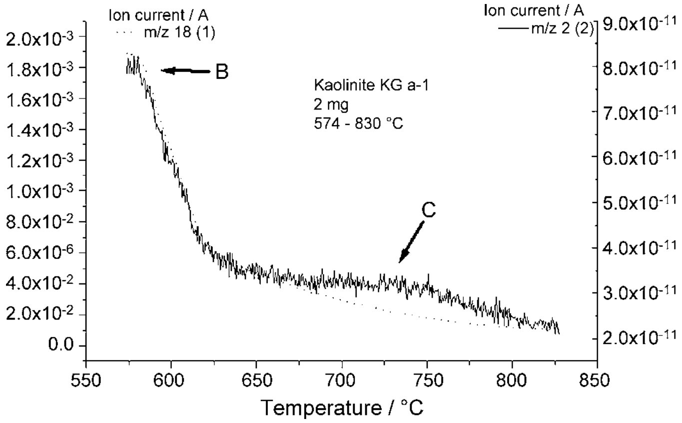

Fig. 6. Degassing intensity of m/z 2 and m/z 18, data from Fig. 3 kaolinite KGa-1 between 574 and 830 °C.

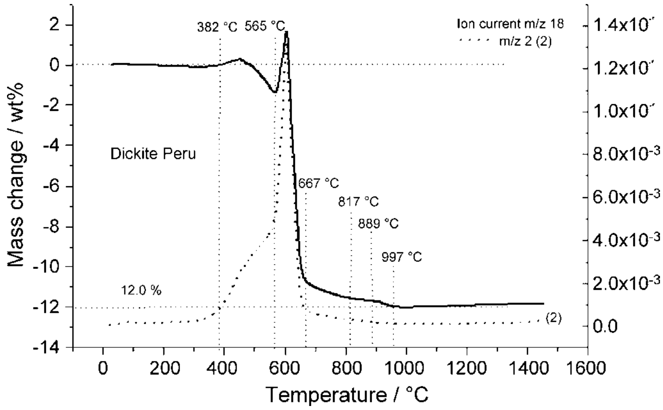

Fig. 7. Mass loss and water release of dickite Peru.

The dickite decomposition shows a clear differentiation in three ranges with different rate of decomposition (Fig. 7):

(1) 382–565 °C	1.40 wt% = 0.20 mol H_2O
(2) 565–667 °C	9.39 wt% = 1.35 mol H_2O
(3) 667–997 °C	1.21 wt% = 0.17 mol H_2O
$\sum$	12.00 wt% = 1.72 mol H_2O

During the exothermic high temperature transformation in any cases also traces of water (≈0.2 wt% ≈0.04 mol H_2O) escape (Fig. 8).

4. Discussion

The vacuum experiments confirm the results in literature [7] that about 0.2 mol water are mobile at room temperature and release from the sample (10 mg) under high vacuum conditions at room temperature within 12 h.

A possible mechanism of the structural change during the beginning of dehydroxylation is schematically illustrated in Fig. 9. Isolate OH-groups, O^-, and vacancies are formed during this process.

$$OH^- + OH^- \rightarrow O^- + H_2O + \square^- \tag{2}$$

O^--ions formed positive holes with respect to the surrounding O^{2-}. This reaction is of importance for the formation of V-

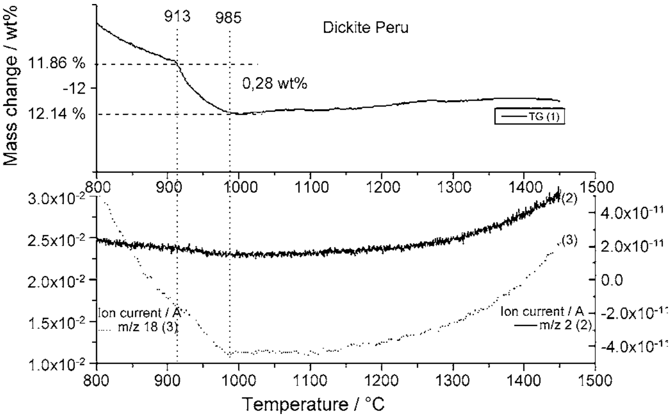

Fig. 8. Water and hydrogen release of dickite Peru in the high temperature range (800–1450 °C).

type centres. Such V-type centres are trapped-hole centres at the surface or in the bulk of the thermal reaction product.

During the further thermal treatment the probability of the formation of H_2O molecules is decreased. The formation of molecular hydrogen was evaluated within a cation vacancy in AlO neighboured by two residual OH^-groups [11]: $[Al–O\ldots H–H\ldots O–Al]^{4+}$. This arrangement is meta-stable at a H–H distance <0.8 Å, close to the H–H distance 0.746 Å in free H_2 molecule [17].

Formally the reaction can be written as:

$$OH^- + OH^- \rightarrow\ 2O^- + H_2 \tag{3}$$

The high mobility of protons makes the formation of hydrogen possible [17].

In order to test the correlation between the degassing rate of both species we plotted m/z 2 against m/z 18 (Fig. 10).

As shown in Table 3 the correlation between the intensity of ion currents of $H_2{}^+$ and H_2O^+ about the total heating range (RT 1450 °C) is 96.86% and the intensity of ion current of $H_2{}^+$ is 0.291% of the intensity of the ion current of H_2O^+.

The correlation of $H_2{}^+/H_2O^+$-ion current relation is decreased in selected temperature ranges compared to the dehydration process of kieserite (Table 2). In the range of low correlation the ratio H_2/H_2O is increased up to 1.852%.

We used the relation of the ion currents of OH^+/H_2O^+ as reference for the water release. As shown in Tables 2 and 3 the intensity of OH^+ is ≈30% of the intensity of H_2O^+, both in kieserite, kaolinite, and dickite with a correlation coefficient >99.8%. This relation is constant in all ranges of decompositions.

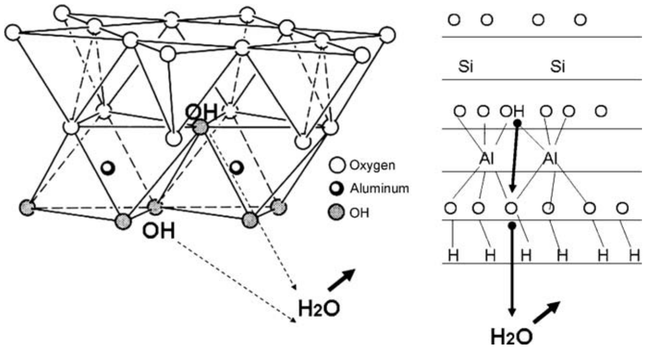

Fig. 9. Schematic illustration of the first step of water release from kaolinite.

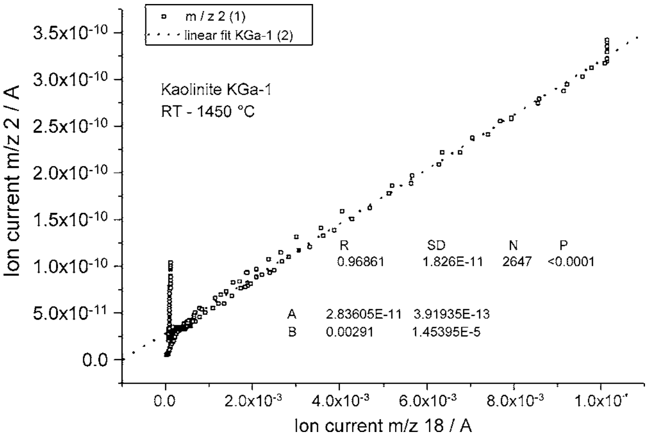

Fig. 10. Linear fitting of the m/z 2 to m/z 18 kaolinite KGa-1. R, correlation coefficient; S.D., standard deviation; N, number of data points; P, probability. A; B = A + Bx.

The significant decreasing of the correlation coefficient and increasing of the relation between the intensities of the ion current of $H_2{}^+$ and H_2O^+ in distinct temperature ranges is an evidence for the hydrogen release in the high temperature range during the decomposition (Fig. 11).

The present results allow making the conclusion that hydrogen was created during the thermal decomposition of kaolinite.

By considering the series of degassing experiments, we can be sure that the formation of H_2 cannot be attributed to instru-

Table 3
The ion current intenisties of $H_2{}^+$ ($m/z = 2$) and OH^+ ($m/z = 17$) in relation to the intensity of H_2O^+ ($m/i = 18 = 100\%$) and the correlation coefficient R

	$H_2{}^+/H_2O^+$ (%)	R (%)	OH^+/H_2O^+ (%)	R (%)
Kieserite	0.34	99.875	29.93	99.998
Kaolinite KGa-1				
RT–1450 °C	0.291	96.86	31.5	99.898
250–426 °C	0.294	99.72	30.332	99.96
450–830 °C	0.293	99.932	–	–
465–602 °C	0.492	99.948	–	–
574–629 °C	0.320	99.62	29.65	99.98
574–830 °C	0.292	98.797	–	–
629–735 °C	0.129	73.588	29.39	99.95
735–828 °C	**0.936**	**92.428**	29.605	99.875
Kaolinite KGa-2				
250–380 °C	0.329	99.493	–	–
436–573 °**C**	0.307	99.953	–	–
573–630 °C	0.302	87.139	–	–
630–735 °C	0.346	84.03	–	–
735–830 °C	**1.852**	**67.112**	29.383	99.603
Dickite Peru				
RT–1000 °C	0.321	99.675	30.86	99.985
293–565 °C	0.323	99.803	–	–
565–608 °C	0.287	99.931	–	–
608–705 °C	0.310	99.924	–	
701–1000 °C	0.399	97.987	29.67	99.965
800–1100 °C	**0.445**	**93.168**	–	

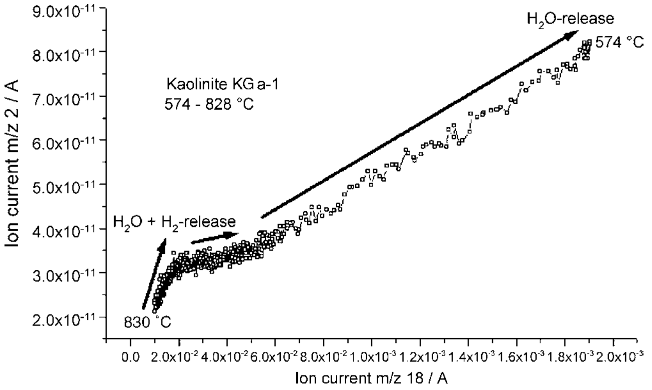

Fig. 11. Plot *m*/*z* 2 as function of *m*/*z* 18 of kaolinite KGa-1 between 574 and 826 °C.

mental artefacts, e.g. as a result of fragmentation of the H_2O molecule.

During the final degassing process the relation changes to a higher content of hydrogen in the evolved gas volume. Therefore we must consider two simultaneous processes during the thermal decomposition:

$$2OH^- \rightarrow O^- + HOH + \square^- > 99\% \qquad (4)$$

$$2OH^- \rightarrow 2O^{2-} + H_2 < 1\% \qquad (5)$$

$\square^-$ = free electron e^-

In respect to the completely different chemical properties of H_2O and H_2 this results suggests a possible hydrogen source during the thermo-metamorphic transformation of kaolinite in a geological process, e.g. during subduction of sedimentary rocks.

The minus difference of about 0.2 mol H_2O is significant in the majority of published data about the decomposition of kaolinite [6,17].

This is an indication for the formation of water from mobile hydrogen before the kaolinite structure collapsed during the heat treatment.

The results confirm the evolution of hydrogen during the dehydroxylation of kaolinite and support a specific structural arrangement of H_2 formation. The three-step decomposition of dickite should be giving more information about the structural processes and requires more detailed study.

In any cases in the high temperature range (>900 °C) a significant step in the weight loss curve gives an indication for the loss of 0.04 mol H_2O (Fig. 8). That means OH-groups can be fixed in the silica structure up to 1100 °C.

The incorporation of CO_2 in kaolinite structure is another interesting fact for the understanding of the solubility and stability mechanism of CO_2 in the earth crust. The correlation to the dehydroxylation (Fig. 12) is an indication for a molecular fixation of CO_2 in the kaolinite structure, perhaps like the "indigenous" carbon in natural goethite [18]. We can also exclude, by the high correlation between the water and CO_2 release, that a mechanical admixture of carbonate minerals (calcite) explains the CO_2 release only. A sure indication for carbonate admixtures is given from the *m*/*z* 44–*m*/*z* 18; plot in Fig. 13.

Furthermore, the occurrence of thermal induced hydrogen and carbondioxides is a further evidence for the structural interaction of sheet silicates with volatiles as were discussed in [17,18].

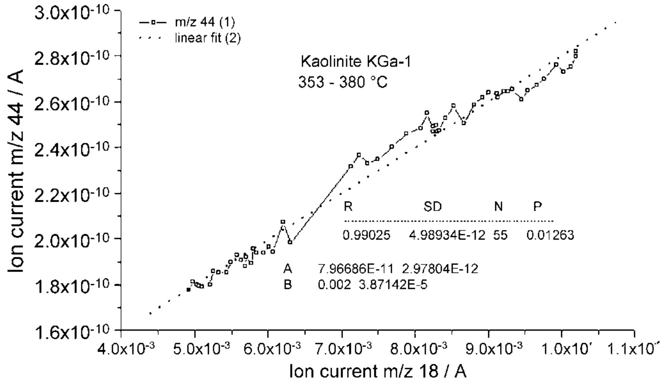

Fig. 12. Plot of CO_2- and water release of Kaolinite KGa-1 between 353 and 380 °C.

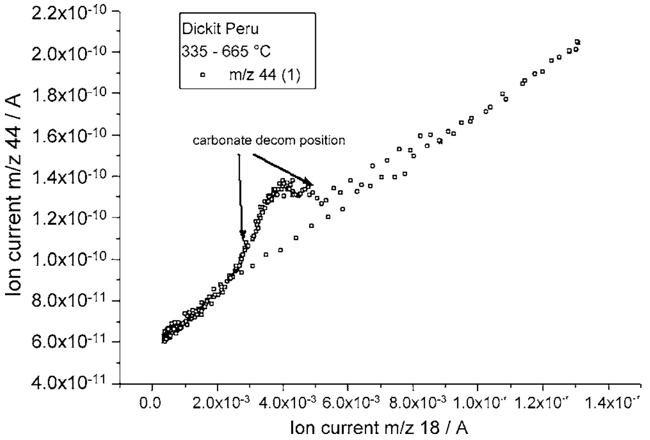

Fig. 13. Degassing intensity of *m*/*z* 44 against *m*/*z* 18 during the decomposition of dickite.

The release of hydrocarbon fragments (*m*/*z* 13 and *m*/*z* 15) is independent of the hydrogen and CO_2-release. Differences between the intensity of *m*/*z* 13 CH^+ and *m*/*z* 15 CH^3 are an indication of the pyrolysis of different hydrocarbon species. *m*/*z* = 15 is a characteristic fragment ion at the pyrolysis of methan (*m*/*z* 16 = CH_4^+). The difference between *m*/*z* 15 and *m*/*z* 13 is an indication of pyrolysis of aliphatic compounds. These results require more detailed studies.

Acknowledgements

We gratefully acknowledge S. Yariv and L. Heller-Kallai, Jerusalem, for offering their helpful discussions and the anonymous referees for the constructive comments.

References

[1] S. Yariv, H. Cross, Organo-Clay Complexes and Interactions, M. Decker, Inc., New York Basel, 2002.
[2] W. Smykatz-Kloss, K. Heide, W. Klinke, Application of Thermal Methods in the Geosciences in Handbook of Thermal Analysis and Calorimetry, vol. 2, Elsevier, 2003.
[3] K.S. Meyers, R.F. Speyer, Application of Thermal Methods in the Geosciences in Handbook of Thermal Analysis and Calorimetry, vol. 2, Elsevier, 2003.

[4] K. Jasmund, G. Lagaly, Tonminerale und Tone, Steinkopf Verlag, Darmstadt, 1993.

[5] J. Hindar, J.L. Holm, J. Lindemann, J. Lǿnvik, Investigation of Some Kaolines by Simultaneous DTA/TG and Thermosonimetry. Thermal Analysis ICTA 80, vol. II, Birkhäuser Verlag, Basel, 1980, pp. 313–318.

[6] R.C. Mackenzie, S. Caillère, Thermal analysis, DTA,TG,DTG, in: H. Van Ophen, J.J. Fripiat (Eds.), Data Handbook for Clay Materials and Other Non-Metallic Minerals, Pergamon Press, Oxford, 1979, pp. 243–284.

[7] W. Smykatz-Kloss, Differential Thermal Analysis, Springer Verlag, 1974.

[8] M. Földvári, J. Therm. Anal. 48 (1997) 107–119.

[9] F. Freund, H. Gentsch, Ber. Dt. Keram. Ges. 44 (1967) 51–58.

[10] F. Freund, W. Gieseke, H. Nägerl, Des processus elementaires de la deshydratation des hydroxides ioniques, in: P. Barret (Ed.), Reaction Kinetics in Heterogeneous Chemical Systems, Elsevier Publ., Amsterdam, 1975, pp. 253–277.

[11] L. Heller-Kallai, I. Miloslavski, A. Grayevsky, Am. Min. 74 (1989) 818–820.

[12] L. Heller-Kallai, J. Therm. Anal. 50 (1997) 145–156.

[13] L. Heller-Kallai, I. Miloslaski, Z. Aizenshtat, L. Halicz, Am. Min. 73 (1988) 376–382.

[14] K. Heide, K. Gerth, E. Hartmann, Thermochim. Acta 354 (2000) 165–172.

[15] J.A. Bain, D. Morgan, Clay Miner. 6 (1969) 171–192.

[16] K. Heide, Dynamische Thermische Analysenmethoden, VEB Deutscher Verlag für Grundstoffindustrie, Leipzig, 1982.

[17] R. Martens, H. Gentsch, F. Freund, J. Catal. 44 (1976) 366–372.

[18] C.J. Yapp, H. Poths, Geochim. Cosmochim. Acta 50 (1986) 1212–1220; L. Wang, M. Zhang, S.A.T. Redfern, Clays Clay Miner. 51 (2003) 439–444.